Theory of highly excited semiconductor nanostructures including Auger coupling: exciton-bi-exciton mixing in CdSe nanocrystals

Marek Korkusinski,[1] Oleksandr Voznyy,[1] and Pawel Hawrylak[1]

[1] *Quantum Theory Group, Institute for Microstructural Sciences, National Research Council, Ottawa, Canada, K1A0R6*

We present a theory of highly excited interacting carriers confined in a semiconductor nanostructure, incorporating Auger coupling between excited states with different number of excitations. The Coulomb matrix elements connecting exciton, bi-exciton and tri-exciton complexes are derived and an intuitive picture of breaking neutral multi-exction complexes into positively and negatively charged multi-exciton complexes is given. The general approach is illustrated by analyzing the coupling of biexciton and exciton in CdSe spherical nanocrystals. The electron and hole states are computed using atomistic $sp^3d^5s^*$ tight binding Hamiltonian including an effective crystal field splitting and surface passivation. For each number of electron-hole pairs the many-body spectrum is computed in the configuration-interaction approach. The low-energy correlated biexciton levels are broken into charged complexes: a hole and a negatively charged trion and an electron and a positively charged trion. Out of a highly excited exciton spectrum a subspace coupled to bi-exciton levels via Auger processes is identified. The interaction between correlated bi-exciton and exciton states is treated using exact diagonalization techniques. This allows to extract the spectral function of the biexciton and relate its characteristic width and amplitude to the characteristic amplitude and timescale of the coherent time evolution of the coupled system. It is shown that this process can be described by the Fermi's Golden Rule only if a fast relaxation of the excitonic subsystem is accounted for.

I. INTRODUCTION

There is currently renewed interest in the understanding of multi-exciton complexes in highly excited semiconductor nanostructures and their interaction with light. Two examples are bi-exciton-exciton cascade for the generation of entangled photon pairs in self-assembled quantum dots[1–5] and enhancing the efficiency of photovoltaic cells by generation of multi-exciton complexes (MEG) from a single, high-energy photon absorbed in semiconductor nanocrystals (NCs).[6–12] While much progress has been achieved in the understanding of multi-exciton complexes in self-assembled quantum dots[13–15] and nanocrystals,[16–32] the mixing and decay of complexes with different numbers of excitons are much less understood.

These processes are important for the understanding of decoherence in entangled photon pairs and energy-to-charge conversion. Nozik[6] has put forward a proposal of converting the energy of the high-energy exciton generated by a high energy photon into several low-energy electron-hole pairs rather than allowing this energy to be dissipated. The theoretical threshold photon energy, at which the excited exciton is expected to convert into a biexciton, depends on the nanocrystal size, but is typically about twice the semiconductor bandgap, $2E_g$. Such carrier multiplication process has been demonstrated in PbSe, PbS, PbTe, CdSe, InAs, and Si NCs,[33,34] with efficiency reaching 700% (seven electron-hole pairs out of one photon).[35] However, a careful analysis of these experiments revised these efficiencies to lower values.[10,23,36]

Coherent coupling of bi-exciton to highly excited exciton can lead to coherent conversion from biexciton to exciton and vice versa. However, phonon-assisted relaxation in the exciton subsystem was suggested to destroy coherence and leads to finite bi-exciton lifetime.[37] Exact theoretical estimation of this lifetime is challenging, as even a realistic computation of single-particle states in NCs is difficult: for example, for a CdSe NC with diameter of 2.5 nm with 304 atoms, in the energy range of $3E_g$ there are approximately $1.58 \cdot 10^5$ exciton and $6.2 \cdot 10^9$ bi-exciton states. As an approximation, one typically starts with the computation of NC single-particle states using the $k \cdot p$[24,25], tight-binding[26–29] or empirical pseudopotential methods.[30–32] Next, one builds the electron-hole pair configurations to be coupled, e.g., the exciton (X) and bi-exciton (XX) of similar energy, and neglects all Coulomb coupling (correlations) within each subsystem. Finally, one computes the Coulomb coupling matrix element between the chosen X and XX configurations and computes the lifetime of the XX state using the Fermi's Golden Rule.[7,9,38–41] As typically there are many X states close in energy to the XX state, one utilizes a quasi-resonant approach, scaling the XX-X transition rate by the density of X states and/or using a "resonance window".[7,9,40–42]

A more advanced approach was presented recently by Witzel *et al.*[43] In this work, a time-dependent evolution of a single-photon excitation coupled coherently with multi-exciton states, considered in the $k \cdot p$ approach, is simulated. Decay of each multiexciton state is accounted for in the relaxation-time approximation. It is shown that the relaxation times of different multiexciton complexes, and in particular that of X, play a crucial role in the efficiency of MEG.

Engineering of materials and nanostructures directed at optimization of the MEG gain requires therefore a comprehensive, microscopic theory of (i) coupling of multiexciton states with different number of excitations, and

(ii) relaxation processes of these multiexciton states. In this work we focus on the former, as the latter requires an additional realistic simulation of the phonon modes in the NC and a treatment of the carrier-phonon coupling.[44,45] We provide a detailed derivation of the Coulomb matrix element coupling the multi-electron-hole configurations differing by one electron-hole pair.[46] Further, we express the states of the system in the basis of configurations with different number of excitations. The form of this expansion is obtained by exact diagonalization of the Hamiltonian accounting for *all* Coulomb interactions of quasiparticles. From such an eigenstate we extract the spectral function of the state with the larger number of pair excitations, assuming that it is "immersed" in a dense spectrum of the states with fewer pairs. To make contact with the language of the state lifetime, used in experiments, we relate the amplitude and the characteristic width of this spectral function to the amplitude and time constants of the coherent time evolution of the system.

We illustrate this framework on the mixing of X and XX in a spherical CdSe nanocrystal. The current work is built upon our recent calculation of the electronic and optical properties of low energy X and XX states in the CdSe NC.[47] We utilize the QNANO computational platform[48] to carry out atomistic tight-binding computation of the single-particle states in the NC with diameter of 3.8 nm. These states are used to construct the *correlated* ground state of the XX as well as the excited states X^* with energies close to that of the XX. From the exact diagonalization of the XX interacting with X^* in this energy range we extract the spectral function of the XX ground state and discuss its properties in connection with the coherent time evolution of the coupled system without relaxation. For the NC studied we find that the XX-X^* coupling is weak, resulting in quantum beats between the XX and X^* states. We demonstrate that contact with the description of the XX population in terms of lifetime can be established only if very fast decay of the X^* states due to phonons is assumed.

The paper is organized as follows. In Section II we present a framework theoretical approach to the system in which the multiexciton states differing in the number of excitations are coupled. We establish the general form of the Hamiltonian for the system, and, on an example of the $X-XX-XXX$ system, demonstrate the derivation of the coupling Coulomb matrix elements. We write the eigenstates of the coupled system, define the spectral function of the system of n electron-hole pairs immersed in the spectrum of $n-1$ and $n+1$-pair excitations, and relate this function to the time evolution of the system. We illustrate these concepts in detail in Section III on the example of the coupled $X-XX$ system confined in a single CdSe nanocrystal. In Section IV we present conclusions and outlook.

II. MODEL

In this Section we present a general derivation of the Coulomb matrix elements which couple the multiexciton configurations differing in the number of electron-hole pairs. We demonstrate how to include these elements in the exact diagonalization study of the mixed system and how to extract physically relevant quantities from that calculation.

A. Derivation of the coupling Coulomb elements

We start the derivation by writing the all-electron Hamiltonian for the semiconductor nanostructure. If by c_i^+ (c_i) we denote the creation (annihilation) operator of an electron on state $|i\rangle$, we have:

$$\hat{H} = \sum_i \tilde{E}_i c_i^+ c_i + \frac{1}{2}\sum_{ijkl}\langle ij|V_{ee}|kl\rangle c_i^+ c_j^+ c_k c_l, \qquad (1)$$

where $\tilde{E}_i$ are the single-particle energies of the nanostructure, while $\langle ij|V_{ee}|kl\rangle$ are the Coulomb scattering matrix elements computed for the single-particle states. Since in the typical NCs we deal with $\sim 10^3$ atoms, or $\sim 10^4$ electrons, we cannot treat the above Hamiltonian directly and introduce the language of quasiparticles. To this end, we divide the basis of single-particle states into two sets: the valence states, henceforth enumerated by Greek indices, and the conduction states, enumerated with Latin indices. As a result, the first term of the above Hamiltonian will split into two, while the Coulomb operator will result in the appearance of $2^4 = 16$ terms. Among these terms there are those which describe the interaction of carriers on conduction states only, as well as that of carriers on valence states only. Further, we find terms describing the interaction between conduction and valence carriers, consisting of the direct and exchange component. Next, we have terms which describe all possibilities of the Coulomb scattering with transfer of one carrier from the valence to conduction band or the other way around. All of them consist of the "direct"-like and "exchange"-like component. Finally, there are terms describing the Coulomb scattering with transfer of *two* carriers, from the valence to conduction band and the other way around. Due to the two-body character of Coulomb interactions, the above Hamiltonian exhausts all possibilities of Coulomb scattering in the system. We shall write all these terms explicitely below.

In order to complete the transition into the language of quasiparticles, we define the "vacuum" reference state of our system, in which all valence orbitals are occupied, and all conduction orbitals are empty:

$$|0\rangle = \prod_\alpha c_\alpha^+ |vac\rangle, \qquad (2)$$

where $|vac\rangle$ denotes the true zero-electron state. The energy of the state $|0\rangle$, E_0, is treated as the reference

level. In what follows, we will consider the charge-neutral electron-hole excitations from that state, which can be written as

$$|i,j,k,\ldots,\alpha,\beta,\gamma,\ldots\rangle = c_i^+ c_j^+ c_k^+ \ldots h_\alpha^+ h_\beta^+ h_\gamma^+ \ldots |0\rangle. \quad (3)$$

Here the hole creation (annihilation) operators are defined as $h_\alpha^+ = c_\alpha$ ($h_\alpha = c_\alpha^+$), respectively. As is evident from the discussion opening this Section, the Hamiltonian (1) describes direct coupling of a configuration with n electron-hole pairs and configurations with $n-2$, $n-1$, n, $n+1$, and $n+2$ pairs. However, we need to translate it into the language of quasiparticle operators. By replacing the valence operators with the hole operators and rearranging terms, we obtain:

$$\hat{H}_{QP} = \hat{H}_{CONS} + \hat{H}_{NC}, \quad (4)$$

where the part conserving the number of excitations is

$$\begin{aligned}\hat{H}_{CONS} &= \sum_i E_i c_i^+ c_i + \frac{1}{2}\sum_{ijkl}\langle ij|V_{ee}|kl\rangle c_i^+ c_j^+ c_k c_l \\ &- \sum_\alpha E_\alpha h_\alpha^+ h_\alpha + \frac{1}{2}\sum_{\alpha\beta\gamma\delta}\langle\delta\gamma|V_{ee}|\beta\alpha\rangle h_\alpha^+ h_\beta^+ h_\gamma h_\delta \\ &- \sum_{i\beta\gamma l}\left(\langle i\gamma|V_{ee}|\beta l\rangle - \langle i\gamma|V_{ee}|l\beta\rangle\right) c_i^+ h_\beta^+ h_\gamma c_l, \quad (5)\end{aligned}$$

and the part changing the number of excitations is

$$\begin{aligned}\hat{H}_{NC} &= \frac{1}{2}\sum_{ijk\delta}\left(\langle ij|V_{ee}|k\delta\rangle - \langle ij|V_{ee}|\delta k\rangle\right) c_i^+ c_j^+ c_k h_\delta^+ \\ &+ \frac{1}{2}\sum_{i\beta kl}\left(\langle i\beta|V_{ee}|kl\rangle - \langle\beta j|V_{ee}|kl\rangle\right) c_i^+ h_\beta c_k c_l \\ &+ \frac{1}{2}\sum_{\alpha\beta\gamma l}\left(\langle\alpha\beta|V_{ee}|\gamma l\rangle - \langle\alpha\beta|V_{ee}|l\gamma\rangle\right) h_\alpha h_\beta h_\gamma^+ c_l \\ &+ \frac{1}{2}\sum_{\alpha j\gamma\delta}\left(\langle\alpha j|V_{ee}|\gamma\delta\rangle - \langle j\alpha|V_{ee}|\gamma\delta\rangle\right) h_\alpha c_j^+ h_\gamma^+ h_\delta^+ \\ &+ \frac{1}{2}\sum_{ij\gamma\delta}\langle ij|V_{ee}|\gamma\delta\rangle c_i^+ c_j^+ h_\gamma^+ h_\delta^+ \\ &+ \frac{1}{2}\sum_{\alpha\beta kl}\langle\alpha\beta|V_{ee}|kl\rangle h_\alpha h_\beta c_k c_l. \quad (6)\end{aligned}$$

In the above Hamiltonian, the single-particle energies are those of quasiparticles, and therefore have to be properly dressed in selfenergy and vertex correction terms. We shall not analyze them in greater detail, as all methods of calculation of the single-particle structure, i.e., $k\cdot p$, tight-binding, or pseudopotential approaches, at some point are fitted to the experimental bandgaps, and therefore are parametrised with already dressed single-particle energies. Note that all Coulomb elements are computed with previous, electron rather than the quasiparticle orbitals. These orbitals are computed directly in the single-particle methods and care must be taken to translate the Coulomb elements into the quasiparticle language. For example, the hole Coulomb matrix element $\langle\alpha\beta|V_{hh}|\gamma\delta\rangle = \langle\delta\gamma|V_{ee}|\beta\alpha\rangle$, that is, it is a complex conjugate of the electron element, while the relation for electron-hole interactions is even more complicated.

The form of the Hamiltonian (4) allows to appreciate the terms changing the number of excitations in a clearer fashion: the terms changing the number of excitations by one have three quasielectron and one hole operators (or conversely), while the terms changing the number of excitations by two are built of four creation or four annihilation operators.

In semiconductor nanostructures the scattering with transfer of one carrier must necessarily modify the energy of a configuration by at least one gap energy E_g, while the transfer of two carriers introduces a modification of at least $2E_g$. The largest mixing of configurations with different numbers of excitations will be seen for configurations close in energy. Therefore, in order to obtain coupling between a low-lying two-pair excitation, or biexciton (XX), and an exciton (X), one has to consider highly excited exciton states (excited by at least E_g).[6] The X-XX-tri-exciton mixing will start at even higher energies (of at least $3E_g$), i.e., both X and XX must be highly excited. We shall describe this case here in a greater detail. Let us first write explicitely the Coulomb matrix elements coupling the X and XX. We couple a one-electron-hole-pair configuration $|X,i\alpha\rangle = c_i^+ h_\alpha^+|0\rangle$ with a two-pair configuration $|XX,jk\beta\gamma\rangle = c_j^+ c_k^+ h_\beta^+ h_\gamma^+|0\rangle$ and obtain:[46]

$$\begin{aligned}\langle XX,jk\beta\gamma|\ \hat{H}_{QP}\ |X,i\alpha\rangle &= \left[\left(\langle jk|V_{ee}|\beta i\rangle - \langle jk|V_{ee}|i\beta\rangle\right)\delta_{\alpha\gamma}\right. \\ &+ \left.\left(\langle jk|V_{ee}|i\gamma\rangle - \langle jk|V_{ee}|\gamma i\rangle\right)\delta_{\alpha\beta}\right] \\ &+ \left[\left(\langle\alpha j|V_{ee}|\gamma\beta\rangle - \langle\alpha j|V_{ee}|\beta\gamma\rangle\right)\delta_{ik}\right. \\ &+ \left.\left(\langle\alpha k|V_{ee}|\beta\gamma\rangle - \langle\alpha k|V_{ee}|\gamma\beta\rangle\right)\delta_{ij}\right] \quad (7)\end{aligned}$$

In the above formula, the terms in the first square bracket apply to the scattering event whereby the creation of an electron-hole pair is accompanied by a scattering of the electron constituting the exciton, while the exciton's hole *must not* change its orbital. The second square bracket contains analogous terms for the case when the exciton's hole is scattered, but its electron must stay on the same orbital. This gives a selection rule for the pair creation process: the exciton and biexciton configurations must share at least one carrier. The process in which the hole is shared is illustrated in the transition Fig. 1(a)-(b). In Fig. 1(a) we show schematically a one-pair configuration, in which the hole occupies the single-particle ground state, while the electron is highly excited. In the scattering process, the electron transfers to a lower single-particle level, while an additional electron-hole pair is created. In Fig. 1(b) this negatively charged trion complex $X-$ is marked with the rectangle, with the empty circle denoting the initial level of the excited electron. Note that the shared hole is a spectator quasiparticle and does not take part in this process. The scattering event with

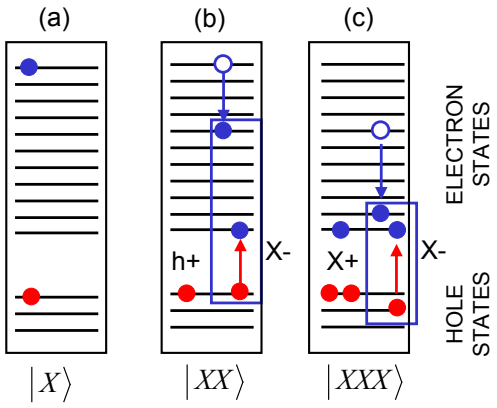

FIG. 1: (Color online) Schematic diagram of the one-pair excitation (a), the two-pair excitation (b), and the three-pair excitation (c). Empty circles denote removed quasiparticles. The negatively charged trion $X-$ appearing as a result of this scattering event is marked with the rectangles.

shared electron would conform to similar rules, only in this case we would deal with a highly excited hole converting to a positively charged trion, while the shared electron would be inert. In the case of the X-XX coupling, the selection rule severely limits the number of excited X configurations to which any XX configuration can couple directly. Henceforth we shall refer to these exciton configurations as X_1^*. However, there are also excited X configurations, which are not directly coupled to the XX configuration, but do couple to X_1^*. These configurations shall be referred to as X_2^*. We shall discuss the importance of X_2^* later on.

Let us now move on to the coupling between the two- and three-pair excitations, whose one variant is visualized schematically in the transition Fig. 1(b)-(c). The matrix element between the two-pair configuration $|XX, jk\beta\gamma\rangle = c_j^+ c_k^+ h_\beta^+ h_\gamma^+ |0\rangle$ and the three-pair configuration $|XXX, lmn\delta\sigma\pi\rangle = c_l^+ c_m^+ c_n^+ h_\delta^+ h_\sigma^+ h_\pi^+ |0\rangle$ is computed similarly to the one connecting the one- and two-pair configurations. We shall not write it here as it is composed of a large number of terms describing various permutations of particles. Let us only emphasize that the scattering process involves a creation of a negatively charged trion $X-$ out of one excited electron, or a positively charged trion out of one excited hole, just as in the case of the X-XX coupling. Figure 1(c) depicts the former, as the excited electron is scattered down the ladder of single-particle states (blue arrow) with a simultaneous creation of the third electron-hole pair (red arrow). The resulting negatively charged trion is denoted in the right-hand panel of Fig. 1(b) by the blue rectangle. The remaining three "spectator" particles are inert and form a positively charged trion $X+$.

Finally, there is also a possibility of coupling the one- and three-pair exictations directly via the two last terms of the Hamiltonian (4). However, in this case the energies of the configurations must necessarily differ by at least $2E_g$. This is why in the following we shall neglect this term.

B. Eigenstates of the mixed system

Presently we solve for the eigenvalues and eigenstates of the system with a non-constant number of excitations. To this end, we use a procedure consisting of two steps. First, we solve for eigenstates and eigenenergies of the Hamiltonian (4) in the subspaces spanned by the configurations with a *conserved* number of excitations. In this case, only the first five terms of that Hamiltonian are considered. We solve this problem in the exact diagonalization approach, in which the Hamiltonian matrix is written in the basis of configurations of the type given in Eq. (3) and diagonalized numerically. As a result of this procedure, for a system with n electron-hole pairs we obtain the eigenstates of the form

$$|nX\rangle_p = \sum_{i,j,\ldots,\alpha\beta\ldots} A^{p,n}_{i,j,\ldots,\alpha\beta\ldots} |i,j,\ldots,\alpha,\beta\ldots\rangle, \qquad (8)$$

where the coefficients $A^{p,n}_{i,j,\ldots,\alpha,\beta\ldots}$ compose the p-th eigenvector of the Hamiltonian matrix, and the energy of this state is $E_{p,n}$. Since the number of possible n-pair configurations can be very large, we restrict the basis to the region of energies of interest and control the convergence of the resulting energy levels with the width of that region.

In the second step, utilizing the energies and eigenstates of systems with conserved excitation numbers, we set up the full matrix of the Hamiltonian (4). The only nondiagonal elements in this matrix will result from the Hamiltonian terms changing the number of excitations. They are computed as linear combinations, which, for example, for the coupled X_1^*-XX system take the form:

$$\begin{aligned} {}_p\langle\ & XX|\hat{H}_{QP}|X_1^*\rangle_q \\ &= \sum_{j,k,\beta,\gamma} \sum_{i,\alpha} \left(A^{p,XX}_{k,l,\beta,\gamma}\right)^* A^{q,X}_{i,\alpha} \langle kl\beta\gamma|\hat{H}_{QP}|i,\alpha\rangle. \end{aligned} \qquad (9)$$

Note that although the individual coupling elements under the sum may vanish due to the selection rule described above, the elements connecting the correlated states may still be finite. We diagonalize the Hamiltonian matrix to obtain the eigenstates with mixed number of

excitations. The K-th state can be written as the linear combination:

$$|K\rangle = B^K|0\rangle + \sum_i \sum_n C^K_{i,n}|nX\rangle_i. \quad (10)$$

The energy of this state is referred to as ε_K.

C. Spectral function and its relation to time evolution

The degree of mixing between states with different number of excitations can be extracted from the eigenstates $|K\rangle$ by calculating the spectral function $A_{p,n}(K)$ of the p-th state with n electron-hole pairs $|nX\rangle_p$. This function is computed as

$$A_{p,n}(K) = |\,{}_p\langle\, nX|K\rangle|^2 \quad (11)$$

and, for example, for the p-th biexciton state will take the form $A_{p,2}(K) = |C^K_{p,2}|^2$, i.e., it is readily obtained from the eigenvectors of the system. For weak coupling we expect that the spectral function will have the value close to 1 for K such that $\varepsilon_K \approx E_{p,n}$, and decay as we move to the other eigenstates $|K\rangle$.

In practice, one is typically interested in the lifetime of the multiexciton state and attempts to engineer the system so as to achieve long lifetimes of states with many excitons. If the dynamics of the system is governed by the Hamiltonian (4) only and is not changed by any incoherent relaxation processes, we can trace the time evolution of the state $|\Psi\rangle$ of the coupled system simply by

$$|\Psi(t)\rangle = \exp\left(-\frac{i}{\hbar}\hat{H}_{QP}t\right)|nX\rangle_p, \quad (12)$$

assuming that the system is prepared in the state $|nX\rangle_p$. Since $|nX\rangle_p = \sum_K \left(C^K_{p,n}\right)^* |K\rangle$, we have

$$|\Psi(t)\rangle = \sum_K \exp\left(-\frac{i}{\hbar}\varepsilon_K t\right)\left(C^K_{p,n}\right)^* |K\rangle, \quad (13)$$

and we can observe the time evolution of our state by computing the projection $|\,{}_p\langle\, nX|\Psi(t)\rangle|^2 = \left|\sum_K \exp\left(-\frac{i}{\hbar}\varepsilon_K t\right)\left|C^K_{p,n}\right|^2\right|^2 = \left|\sum_K \exp\left(-\frac{i}{\hbar}\varepsilon_K t\right) A_{p,n}(K)\right|^2$. The time evolution of the system, and in particular the change of the number of excitations from the one prepared in the system, is related to the Fourier transform of the spectral function in the time domain. At this point it is useful to consider two limiting examples of the spectral function. First, if $A_{p,n}(K)$ is finite only for several states K, we may expect a complex time evolution, with oscillating contributions from all these states.

Second, if our state $|nX\rangle_p$ is immersed in a quasi-continuous spectrum of other states (possibly with different n) and if its spectral function can be approximated by a Lorentzian, $A_{p,n}(K) \approx (\gamma/2\pi)/[(\varepsilon_K - E_{p,n})^2 + (\gamma/2)^2]$ and $A_{p,n}(K) = A_0$ on resonance, then the time evolution is described by an exponential decay, $|\,{}_p\langle\, nX|\Psi(t)\rangle|^2 = |A_0 + (1-A_0)\exp(-\gamma t/2)|^2$, with γ being the characteristic width of the spectral function. At long times and with strong mixing (the value of $A_0 \ll 1$), the state of the system can no longer be identified with the state $|nX\rangle_p$, as the probability density is distributed *coherently* in the multitude of states of the system. The above analysis shows that the characteristic decay time constant $1/\gamma$ is *not* related simply to the bare coupling between the state $|nX\rangle_p$ and other states *at the same energy*, as this will predominantly affect the spectral function maximum value A_0. The dynamics of this "dissolution" of our state $|nX\rangle_p$ is decided by its coupling to states off-resonance: the stronger that coupling, the broader the spectral function and the faster the decay. Note also that the probability of finding the system in the state $|nX\rangle_p$ does not decay to zero, but rather the amplitude A_0^2. We shall supplement this intuitive picture with a detailed analysis of the dynamics in the next Section.

III. EXCITON-BIEXCITON COUPLING IN CDSE NANOCRYSTALS

In this Section we apply the general approach to describing the dynamics of the bi-exciton XX in a CdSe nanocrystal with diameter of 3.8 nm, as studied in Ref. 47. We choose to focus on the low-energy XX states, which allows us to consider their coupling only to excited exciton states of similar energy. Below we will discuss the entire procedure, starting from the computation of single-particle states, then the correlated states of X and XX, coupling matrix elements, treatment of the mixed system and extraction and analysis of the spectral function.

A. Single-particle states

We start the parametrization of the Hamiltonian (4) with the computation of single-particle states and their energies. To this end we utilize the atomistic tight-binding sp^3d^5s* approach. We look for the single-particle wave function $|i\rangle$ in the form of a linear combination

$$|i\rangle = \sum_{R,\alpha} F^{(i)}_{R,\alpha}|R,\alpha\rangle \quad (14)$$

of atomic orbitals $|R,\alpha\rangle$. The index α enumerates the types of orbitals (s, three p, five d, and $s*$, of which all are degenerate spin-doublets), while the index R enumerates atoms. The coefficients $F^{(i)}_{R,\alpha}$ and the energies E_i of states are computed by diagonalizing the tight-binding Hamiltonian

$$\hat{H}_{TB} = \sum_{R,\alpha} \varepsilon_{R,\alpha} c^+_{R,\alpha} c_{R,\alpha} + \sum_{R,\alpha,\beta} \lambda^{SO}_{R,\alpha,\beta} c^+_{R,\alpha} c_{R,\beta}$$

$$+ \sum_{R,\alpha} \sum_{R',\beta} t_{R,\alpha}^{R',\beta} c_{R,\alpha}^{+} c_{R',\beta} \qquad (15)$$

written in the basis of atomic orbitals. This Hamiltonian is parametrized by the on-site energies $\varepsilon_{R,\alpha}$, spin-orbit parameters $\lambda_{R,\alpha,\beta}^{SO}$, and hopping elements $t_{R,\alpha}^{R',\beta} c_{R,\alpha}^{+}$. These parameters are established by fitting the bulk band structure obtained with the above Hamiltonian to the structure obtained either with *ab initio* methods or experimentally.[47] In Ref. 47 we have presented an extensive analysis of the electronic and optical properties of NCs using the atomistic tight-binding method. Here we will summarize it briefly.

We focus on the spherical CdSe nanocrystal with diameter of 3.8 nm. The underlying crystal lattice of the NC is of the wurtzite modification. The lattice symmetry induces the crystal field, whose effects are apparent only at the third-nearest neighbor distances, and therefore are not treated naturally with the nearest-neighbor Hamiltonian (15). We model the crystal field by introducing a splitting in energies of the p orbitals on each atom. The NC surface is passivated in a model approach by applying a large energy shift to any dangling bond.[49] The sample is composed of 10^3 atoms, which results in the tight-binding Hamiltonian matrix of $2 \cdot 10^4$. Since in our further analysis we require single-particle states whose energies fall into a large region (approximately from $-2E_g$ to $2E_g$), we perform the diagonalization of our Hamiltonian using full-matrix diagonalization tools.

The energies of several lowest-lying electron and hole states are visualized in Fig. 2(a). Here, bars represent the energies of Kramers doublets, which are degenerate due to the time-reversal symmetry. The electron states correspond well with those of a spherical quantum well, with a single s-like level and three quasi-degenerate p-like levels about 270 meV higher. The hole states, on the other hand, form a low-energy, quasi-degenerate shell composed of four Kramers doublets, separated from the rest of the spectrum by a gap of about 120 meV. The complicated structure of the hole states is a consequence of the spin-orbit interactions and the presence of the crystal field.

In order to complete the construction of the quasiparticle Hamiltonian (4), we need to compute all relevant Coulomb matrix elements using the single-particle TB wave functions. We use the expansion, in which we separate the on-site terms arising from the scattered particles residing on the same atom and the long-distance terms describing scattering between more remote atoms.

$$\begin{aligned} \langle ij|V_{ee}|kl\rangle &= V_{ons} + V_{long}, \qquad (16) \\ V_{ons} &= \sum_{R} \sum_{\alpha\beta\gamma\delta} F_{R,\alpha}^{(i)*} F_{R,\beta}^{(j)*} F_{R,\gamma}^{(k)} F_{R,\delta}^{(l)} \\ &\times \langle R,\alpha,R,\beta| \frac{e^2}{\epsilon_{ons}|\vec{r}_1 - \vec{r}_2|} |R,\gamma,R,\delta\rangle \qquad (17) \\ V_{long} &= \sum_{R_i} \sum_{R_j}^{remote} \sum_{\alpha\beta} F_{R_i,\alpha}^{(i)*} F_{R_j,\beta}^{(j)*} F_{R_j,\beta}^{(k)} F_{R_i,\alpha}^{(l)} \end{aligned}$$

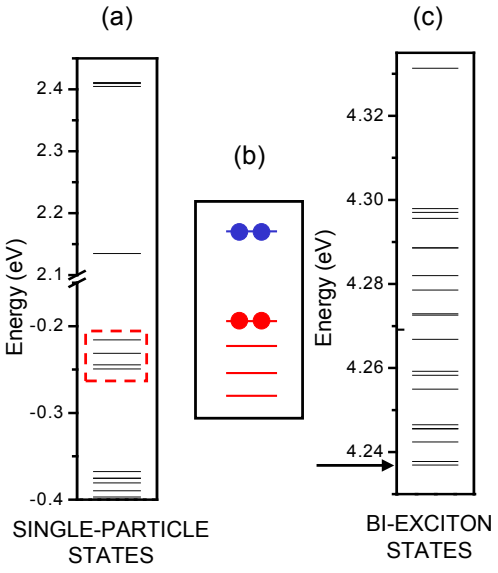

FIG. 2: (Color online) (a) Energies of several lowest-lying single-particle electron and hole states of a CdSe spherical nanocrystal with the diameter of 3.8 nm. Bars denote Kramers doublets. (b) Schematic representation of the dominant two-pair configuration of the lowest bi-exciton state. Arrows distinguish the states within each Kramers doublet. (c) Lowest-energy segment of the bi-exciton spectrum. Arrow denotes the lowest XX state.

$$\times \frac{e^2}{\epsilon_{long}|\vec{R}_i - \vec{R}_j|}. \qquad (18)$$

The integrals scaling the onsite terms are computed by approximating the atomistic functions $|R,\alpha\rangle$ by Slater orbitals.[50] In an attempt to simulate the distance-dependent dielectric function,[31,51–54] each of these terms is scaled by a different dielectric constant ϵ. Typically we take $\epsilon_{ons} = 1$. As for the long-distance term, if the two atoms in question are nearest neighbors, we take $\epsilon_{long} = 2.9$, while for more remote pairs we take $\epsilon_{long} = 5.8$, the latter one being the bulk CdSe dielectric constant.

B. Biexciton and excited exciton

Next we populate the single-particle states with electron-hole pairs. Since the energy range of interest for the exciton-bi-exciton coupling is defined by the energies of XX states, we start with considering the two-electron-hole-pair configurations

$$|i,j,\alpha,\beta\rangle = c_i^{+} c_j^{+} h_\alpha^{+} h_\beta^{+} |0\rangle. \qquad (19)$$

We stress that the quasihole single-particle wave functions are obtained by applying a complex conjugate to the valence functions obtained from diagonalization of the tight-binding Hamiltonian. We build the matrix of the many-body Hamiltonian (4) in the basis of these configurations and diagonalize it numerically. We have presented an extensive study of the electronic and optical properties of XX in Ref. 47. We found that the XX eigenstates have a correlated character, which is due to the gaps between the single-particle hole states being of the same order as the Coulomb scattering matrix elements between the two-pair configurations (tens of meV). By constraining the two electrons to occupy the s-shell electron orbital and distributing the holes among the 4 double-degenerate states of the hole shell [marked in Fig. 2(a) with a red rectangle] we obtain 28 two-pair configurations which mix with each other strongly. The configuration of the four carriers with the lowest single-particle energy is shown schematically in Fig. 2(b). However, the basis restricted to these configurations only is not sufficient to obtain convergence of the XX energies. A satisfactory spectrum of XX energies, shown in Fig.2(c), is obtained only when the electrons are allowed to populate the s- and p-shell single-particle orbitals, while holes are allowed to spread on 14 lowest-energy Kramers doublets. This results in 10976 two-pair configurations. Inclusion of the mixing between the two-pair configurations decreases the XX ground-state energy to the value of $E_{1,2} = 4.237$ eV, that is, by about 75 meV with respect to the uncorrelated case.

In Fig. 2(c) we show only the XX correlated states built predominantly from the original 28 two-pair configurations. The respective XX eigenstates are linear combinations of all basis states, represented in general by Eq. (8) and in this case taking the form

$$|XX\rangle_p = \sum_{i,j,\alpha,\beta} A^{p,XX}_{i,j,\alpha,\beta} |i,j,\alpha,\beta\rangle. \qquad (20)$$

However, these states are typically dominated by one configuration. In Fig. 2(b) we show the two-pair configuration dominant in the lowest-energy XX state. The segment of the spectrum built upon the lowest-shell configurations is separated from the rest of XX states by a gap resulting from the gap in the hole single-particle spectrum. This defines a region of energies appropriate for the studies of X-XX mixing. In what follows, we shall construct the excited exciton configurations, whose energy falls within the window of 4.0 to 4.35 eV, that is, that corresponding to the lowest XX band enlarged from each side by about 0.25 eV.

Let us now describe the procedure of generation of the excited X states. As was explained in Section II A, in order to be able to couple, a two-pair configuration and an excited one-pair configuration have to share at least one carrier. Figure 3 shows how such X_1^* configurations are created assuming that they share a hole (a) or an electron (b) with a two-pair configuration. In this way, from each two-pair configuration one can generate families of

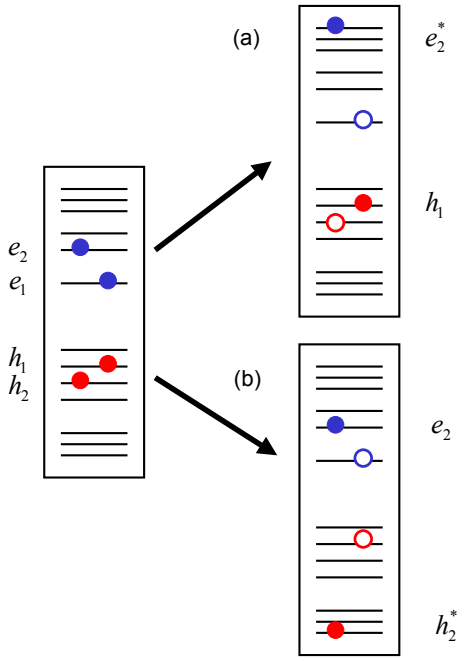

FIG. 3: (Color online) Schematic representation of the allowed Coulomb scattering mechanism connecting the two-pair and one-pair configurations. Empty circles denote removed quasiparticles. Panels (a) and (b) show respectively the event in which the electron and hole are scattered.

X_1^* one-pair configurations and select only those, whose energy falls in the chosen window, as described above. However, generating all eligible X_1^* from all 10976 two-pair configurations would result in a prohibitive size of the X_1^* space. Therefore, we only generate the X_1^* families from the 28 lowest-shell configurations.

The next step is to compute all relevant Coulomb matrix elements between configurations as defined by Eq. (7). As an example, in Fig. 4 we show the absolute values of elements connecting the lowest-energy two-pair configuration with the X_1^* configurations which share a common hole (see a schematic diagram in the inset to this Figure). We see that the elements fall into two categories. Some elements have values ranging from 10^{-6} eV to $2 \cdot 10^{-4}$ eV, while other elements are of 10^{-9} eV and less. We find a similar distribution of the values of matrix elements for X_1^* configurations which share a common electron with the two-pair configurations. The elements from the second category are within the numerical noise of our computation and should be treated as zero, although they quantify an allowed coupling process. The source of such a large disparity of magnitudes of these elements lies in the character of the wave function of the excited electron, promoted to a high orbital due to the scattering. In Fig. 5 we show the single-particle probability densities of the orbitals which participate in the scattering. The electron is promoted from the s-type or-

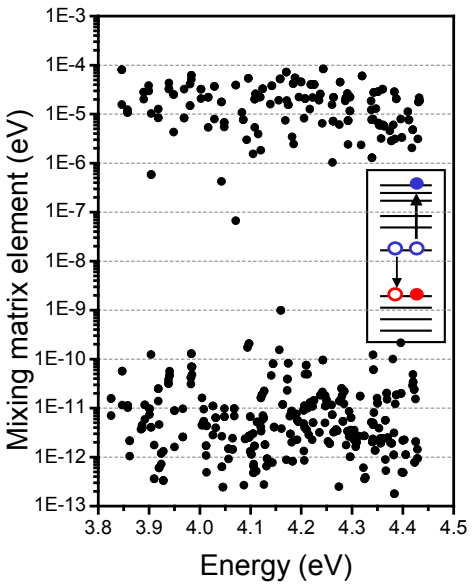

FIG. 4: (Color online) Magnitudes of the Hamiltonian matrix element coupling the lowest-energy bi-exciton configuration [shown in Fig. 2(b)] with single-pair configurations with excited electron, as a function of the energy of these configurations. Inset shows a schematic illustration of the scattering process.

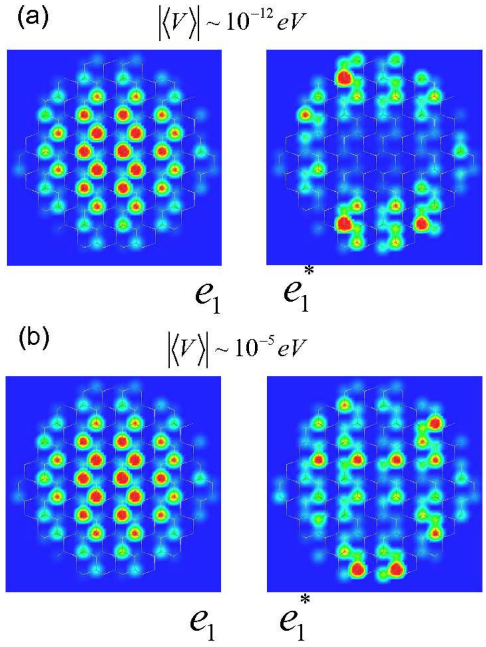

FIG. 5: (Color online) Cross-sectional view of the probability density of electronic states taking part in the scattering process depicted in Fig. 4. The left-hand images correspond to the electron wave function on the s orbital, while the right-hand images characterize the wave functions of the final state. Due to the distribution of the probability density, the element corresponding to the situation (a) is negligible, while that corresponding to the situation (b) is finite.

bital (left) onto one of the highly excited orbitals (right). In the case (a) we find that the final orbital is distributed in an outermost layer of fully-coordinated Cd atoms of the nanocrystal such that the overlap with the tightly confined s orbital is small. This results in a negligible coupling. On the other hand, in the case (b) the overlap between the relevant orbitals appears to be more substantial, resulting in a much larger coupling of 10^{-5} eV. Note that all these matrix elements are at least two orders of magnitude smaller than those connecting different two-pair configurations to each other.[47]

C. Spectral function and dynamics of XX

We now proceed to computing the electronic properties and dynamics of the coupled XX-X system. According to the procedure described in Section II B, having diagonalized the XX subsystem separately, we should now perform a separate diagonalization of the X subsystem and then connect the two. We found, however, that a more computationally efficient procedure involves writing the entire Hamiltonian (4) in the basis of the single-pair and two-pair configurations. This is due to the fact that in such large bases, the calculation of elements (9) coupling correlated X_1^* and XX states takes a very long time.

In order to be able to compute the spectral function, we require all the eigenstates of the coupled system. This sets another limit of the basis size, which, by necessity, was chosen to be about 11000 basis states: 1000 of the two-pair, and 10000 of the single-pair configurations. As a result, the eigenstates of the coupled system, defined in Eq. (10), can be written as

$$|K\rangle = \sum_{i,j,\alpha,\beta} C^K_{i,j,\alpha,\beta}|i,j,\alpha,\beta\rangle + \sum_{i,\alpha} D^K_{i,\alpha}|i,\alpha\rangle. \qquad (21)$$

while the pure XX states are described by Eq. (20). Since the spectral function is defined in terms of a projection of one of the XX states onto the spectrum $|K\rangle$, in this case we have:

$$A_{p,XX}(K) = |\,{}_1\langle\, XX|K\rangle|^2 = \left| \sum_{i,j,\alpha,\beta} \left(A^{p,XX}_{i,j,\alpha,\beta}\right)^* C^K_{i,j,\alpha,\beta} \right|^2 . \qquad (22)$$

In Fig. 6 we plot the spectral function $A_{1,XX}(K)$ of the XX ground state ($p = 1$) as a function of the energy of the eigenstates of the coupled system. The red vertical lines represent the XX (i.e., not mixed with X_1^*) eigenstates, while the gray vertical lines denote the energies $\varepsilon(K)$ of

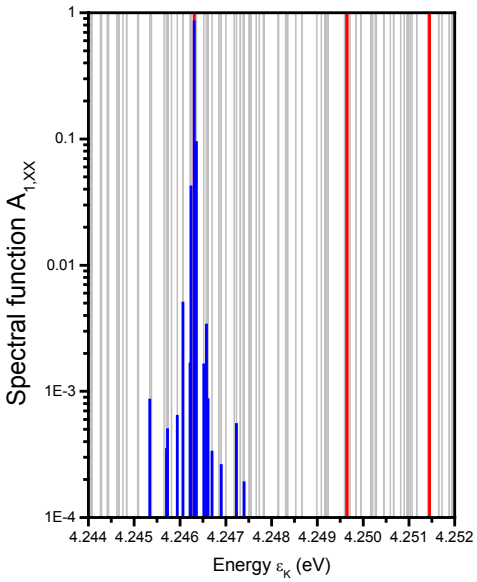

FIG. 6: (Color online) Spectral function of the bi-exciton immersed in the spectrum of exciton states. Red lines indicate the energies of the bi-exciton eigenstates, while gray lines correspond to the exciton eigenstates. Blue bars represent the values of the spectral function of the lowest-energy bi-exciton for each eigenstate of the coupled system.

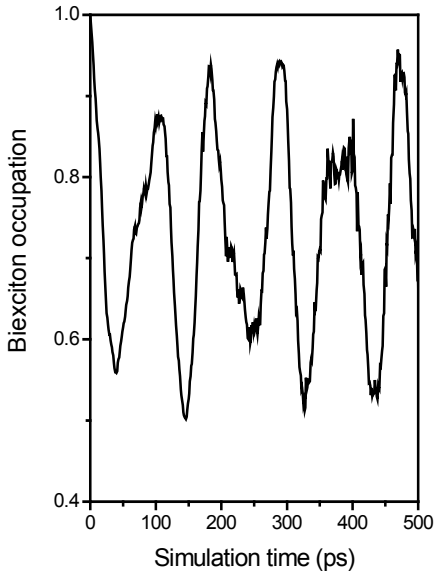

FIG. 7: (Color online) Time evolution of the probability of finding the coupled bi-exciton-exciton system in the ground bi-exciton state.

the mixed eigenstates $|K\rangle$. The values of the spectral functions for different K are represented by the height of the blue bars. We find that the value of the spectral function is 0.847 at the energy corresponding to that of the unmixed XX ground state, and smaller by about an order of magnitude at the energy corresponding to the next state $|K\rangle$. Its value falls off very fast as we move away from this energy, becoming negligibly small already at about 1 meV away. We conclude that our XX level is coupled very weakly to the underlying spectrum of the X_1^* states and is not resonant with any of them.

Next we examine how this weak coupling translates into the dynamics of the coupled system. We assume that the system is prepared in the XX ground state and simulate its time evolution as described in Section II C. The resulting probability of finding the system in the state $|XX\rangle_1$ at time t is plotted in Fig. 7. We find that this probability oscillates around the value of $|A_{1,XX,max}|^2 = 0.72$ with no appreciable decay. The oscillations are not regular, as there are several states which are effectively coupled to $|XX\rangle_1$ and the values of coupling elements vary strongly from state to state. It is clear, however, that we cannot define the XX lifetime in our system in a meaningful fashion.

D. Bi-exciton decay and lifetime

The treatment of our system in terms of the coherent evolution of weakly coupled multiexciton states does not reflect the experimental situation, in which finite lifetimes, of order of tens of picoseconds, are found.[8,11,39,42] In Section II C we have demonstrated that we can obtain a population of the multiexciton state which decays in time even within the coherent model if its spectral function is sufficiently broad. In our system, such broadening can occur as a result of mixing of the X_1^* one-pair configurations, which can be directly coupled to the two-pair configurations, and the X_2^* one pair configurations, which exhibit no such coupling. To account for this mixing, however, we would have to generate *all* the single-pair configurations with energies falling into the chosen energy window. This results in prohibitively large basis sizes. The second broadening mechanism involves relaxation of the one-pair configurations due to phonons. Such relaxation is not relevant for the XX subsystem, as we focus on the XX ground state only. Coherent simulations of the time evolution of such a system have been reported,[43] however there the electronic structure was computed within the four-band $k \cdot p$ approach. Our simulations on model systems indicated that if the relaxation times of the single-pair states are very short, the dynamics of the biexciton can be described by a single lifetime

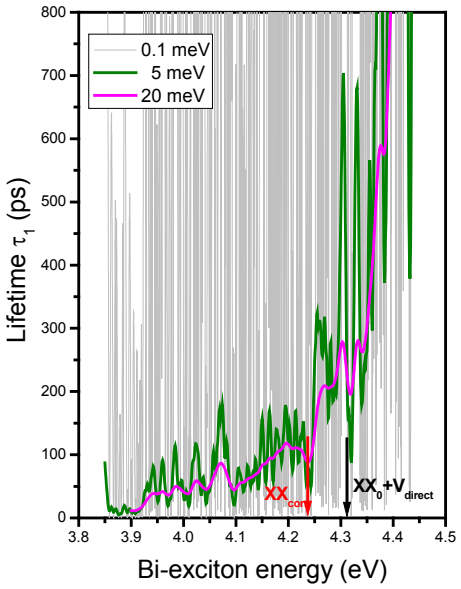

FIG. 8: (Color online) Lifetime of the bi-exciton in the coupled bi-exciton-exciton system computed using the Fermi's Golden Rule with the broadening $\Gamma = 0.1$ meV (gray), 5 meV (green), and 20 meV (magenta). Both exciton and bi-exciton states are uncorrelated.

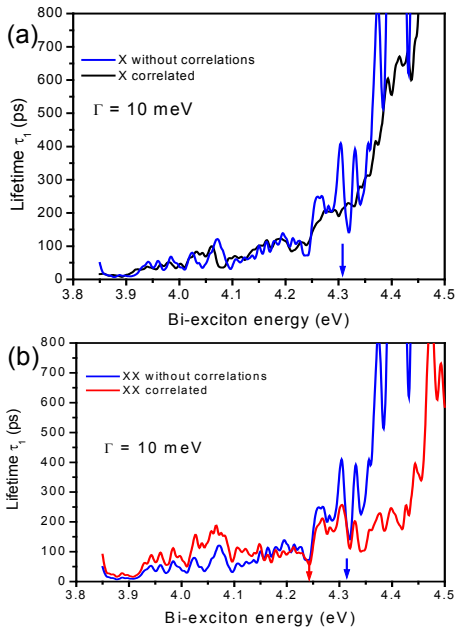

FIG. 9: (Color online) Lifetime of the bi-exciton in the coupled bi-exciton-exciton system computed using the Fermi's Golden Rule assuming that the exciton is correlated and bi-exciton is not (a) and conversely (b).

obtained using the Fermi's Golden Rule[7,9,38–41]

$$\frac{1}{\tau_1} = \frac{2\pi}{\hbar} \sum_i |\, {}_1\langle\, XX|V_{ee}|X\rangle_i|^2 \delta(E_{1,XX} - E_{i,X}), \quad (23)$$

where $E_{1,XX}$ is the ground state energy of the biexciton state and $E_{i,X}$ is the energy of the i-th exciton state. The influence of scattering and relaxation processes is introduced into this rule by broadening the delta function such that $\delta(E_{1,XX} - E_{i,X}) \to (\Gamma/2\pi)/[(E_{1,XX} - E_{i,X})^2 + (\Gamma/2)^2]$, where Γ is a model broadening. In an attempt to model fast relaxation processes, one typically chooses Γ to be sufficiently large so that the result of the calculation does not depend on it.

To make contact with previous work,[7,9,38–41] we begin by assuming that the states $|XX\rangle_1$ and $|X\rangle_i$ are uncorrelated and are simply represented by the two-pair and one-pair configurations, respectively. The single-pair energies are computed as the respective expectation values of the quasi-particle Hamiltonian (4): $E_{i,X} = {}_i\langle\, X|\hat{H}_{QP}|X\rangle_i$. On the other hand, we treat the XX energy $E_{1,XX}$ as an independent variable, whose value will be tuned artificially in order to examine the values of lifetimes over an energy region. However, to compute the matrix element we always use the XX ground state.

In Fig 8 we show the lifetimes computed as a function of the biexciton energy for four broadenings Γ. The actual ground-state energy of the uncorrelated XX is marked with the black arrow, while the energy corresponding to the fully correlated XX is denoted by the red arrow. We find that for a small broadening of $\Gamma = 0.1$ meV, the lifetime as a function of the XX energy exhibits very fast oscillations over many orders of magnitude. Increasing the broadening leads to averaging of these oscillations and an emergence of a monotonic dependence of τ_1 on $E_{1,XX}$. This dependence seems to be converged for $\Gamma = 20$ meV. We find that the lifetime increases with the energy, which is consistent with the decrease of the coupling element with energy (see Fig. 4). In general, we find that depending on the biexciton energy the calculated lifetimes can vary from about 50 ps to about 800 ps. As we change the XX energy from its uncorrelated to correlated value, the lifetime changes by a factor of 3. It is clear, therefore, that accounting for correlations in the many-body states is of crucial importance.

Finally, we examine how the XX lifetime changes if we also include correlations in the many-body states, i.e., depending upon how we compute the coupling matrix element in the Fermi's Golden Rule. Figure 9 shows the lifetime as a function of energy assuming that the X states are correlated while the XX state is not (a) and the other way around (b). Preparation of the X states in their correlated form does not introduce any drastic changes into the lifetime. These correlations can be modeled essentially by an additional broadening in the density of states of single-pair configurations. On the other

hand, introducing correlations into the XX ground state increases the lifetime by about a factor of 2 for lower energies, while for higher energies the lifetime is reduced by a factor of 5. Clearly, the XX lifetime strongly depends on the details of the sample and its coupling with relaxation mechanisms. Detailed *ab initio* studies of the nanocrystal electronic structure and coupling with phonons are necessary to obtain predictions of the lifetime which could be compared to the experimental data.

IV. CONCLUSIONS AND OUTLOOK

In conclusion, we have presented a theory of the coupling between states with different numbers of electron-hole excitations in semiconductor nanostructures. We have derived the appropriate quasiparticle Hamiltonian and demonstrated that the states are coupled by a Coulomb interaction element. This element accounts for the process whereby one electron-hole pair is annihilated and another carrier is scattered within the same band. We have shown that these processes involve the creation or collapse of a charged trion, while the remaining particles act as spectators. The general Hamiltonian for such a coupled system can be diagonalized exactly in the basis of states with different number of excitations. The spectral function of the state with higher number of pairs among the states with fewer pairs was calculated and shown to be related to the time-dependent evolution of the system by the Fourier transform.

This methodology was applied to analyzing the dynamics of the bi-exciton (XX) state immersed in the excited exciton (X) states of similar energy confined in a CdSe spherical nanocrystal. The NC single-particle energies and states were computed within the sp^3d^5s* tight-binding approach and the Coulomb scattering matrix elements were obtained with these atomistically resolved wave functions. We derived the spectral function of the XX ground state immersed in the excited exciton states for an example nanoscrystal of 3.8 nm diameter. We found that the ground XX state is coupled only to a few X^* states close to it in energy. This property was reflected in the time evolution of the state of the coupled system, which involved clear coherent oscillations in the population of the XX state without decay. Lifetime of the XX state could be defined only by introducing additional coupling of excited exciton states and their nonradiative decay mediated by phonons. The exciton-phonon coupling was accounted for in a model fashion by broadening the resonance condition in the Fermi's Golden Rule treatment of the XX lifetime. We found that the lifetime is very sensitive to that broadening (characteristic relaxation times), if the broadening itself is small, but has a convergent behavior for large broadenings. On the other hand, a large change in the XX lifetime was seen when the correlated character of the XX state was accounted for. To investigate this dependence further, we plan to improve on the elements of our approach which were carried out in a model fashion: treatment of surface, a simplified treatment of the distance-dependent dielectric function, and the approximate treatment of relaxation mechanisms of the excited exciton states. Such an approach could be used to provide more quantitative estimates of XX lifetime in NCs.

Acknowledgment

The Authors are grateful to the NRC-NSERC-BDC Nanotechnology Project and the NRC-CNRS grant for financial support.

[1] R.M. Stevenson, R.J. Young, P. Atkinson, K. Cooper, D.A. Ritchie, and A.J. Shields, Nature (London) **439,** 179 (2006).
[2] N. Akopian, N.H. Lindner, E. Poem, Y. Berlatzky, J. Avron, D. Gershoni, B.D. Gerardot, and P.M. Petroff, Phys. Rev. Lett. **96,** 130501 (2006).
[3] A. Greilich, M. Schwab, T. Bestermann, T. Auer, R. Oulton, D.R. Yakovlev, M. Bayer, V. Stavarache, D. Reuter, and A. Wieck, Phys. Rev. B **73,** 045323 (2006).
[4] M.E. Reimer, M. Korkusinski, D. Dalacu, J. Lefebvre, J. Lapointe, P.J. Poole, G.C. Aers, W.R. McKinnon, P. Hawrylak, and R.L. Williams, Phys. Rev. B **78,** 195301 (2008).
[5] M. Korkusinski, M.E. Reimer, R.L. Williams, and P. Hawrylak, Phys. Rev. B **79,** 035309 (2009).
[6] A.J. Nozik, Physica E **14,** 115 (2002).
[7] E. Rabani and R. Baer, Nano Lett. **8,** 4488 (2008).
[8] R.D. Schaller, J.M. Pietryga, V.I. Klimov, and V.I. Carrier, Nano Lett. **7,** 3469 (2007).
[9] A. Franceschetti, J.M. An, and A. Zunger, Nano Lett. **6,** 2191 (2006).
[10] G. Nair and M.G. Bawendi, Phys. Rev. B **76,** 081304 (2007).
[11] R.J. Ellingson, M.C. Beard, J.C. Johnson, P. Yu, O.I. Micic, A.J. Nozik, A. Shabaev, and A.L. Efros, Nano Lett. **5,** 865 (2005).
[12] G.D. Scholes and G. Rumbles, Nature Materials **5,** 683 (2006); *ibid.,* 920 (2006).
[13] L. Jacak, P. Hawrylak, and A. Wojs, *Quantum Dots,* Springer, Berlin, 1998.
[14] D. Bimberg, M. Grundmann, and N.N. Ledentsov, *Quantum Dot Heterostructures,* Wiley, Chichester, 1999.
[15] *Single Quantum dots: Fundamentals, Applications, and New Concepts,* edited by Michler, P., *Topics in Applied Physics,* Vol. 90 (Springer-Verlag, Berlin, 2003).
[16] R. Osovsky, D. Cheskis, V. Kloper, A. Sashchiuk, M. Kroner, and E. Lifshitz, Phys. Rev. Lett. **102,** 197401 (2009).
[17] H. Htoon, S.A. Crooker, M. Furis, S. Jeong, Al.L. Efros, and V.I. Klimov, Phys. Rev. Lett. **102,** 017402 (2009).
[18] M. Furis, H. Htoon, M.A. Petruska, V.I. Klimov, T. Brrick,

and S.A. Crooker, Phys. Rev. B **73,** 241313(R) (2006).
[19] M. Achermann, J.A. Hollingsworth, and V.I. Klimov, Phys. Rev. B **68,** 245302 (2003).
[20] J.-M. Caruge, Y. Chan, V. Sundar, H.J. Eisler, and M.G. Bawendi, Phys. Rev. B **70,** 085316(2004).
[21] C. Bonati, M.B. Mohamed, D. Tonti, G. Zgrablic, S. Haacke, F. van Mourik, and M. Chergui, Phys. Rev. B **71,** 205317 (2005).
[22] V.I. Klimov, S.A. Ivanov, J. Nanda, M. Achermann, I. Bezel, J.A. McGuire, and A. Piryatinsky, Nature **447,** 441 (2007).
[23] S.L. Sewall, A. Franceschetti, R.R. Cooney, A. Zunger, and P. Kambhampati, Phys. Rev. B **80,** 081310 (2009).
[24] A.I. Ekimov, F. Hache, M.C. Schanne-Klein, D. Ricard, C. Flytzanis, I.A. Kudryavtsev, T.V. Yazeva, A.V. Rodina, and Al.L. Efros, J. Opt. Soc. Am. B **10,** 100 (1993).
[25] Al.L. Efros, M. Rosen, M. Kuno, M. Nirmal, D.J. Norris, and M. Bawendi, Phys. Rev. B **54,** 4843 (1996).
[26] K. Leung, S. Pokrant, and K.B. Whaley, Phys. Rev. B **57,** 12291 (1998).
[27] P. Chen and K.B. Whaley, Phys. Rev. B **70,** 045311 (2004).
[28] S. Sapra and D.D. Sarma, Phys. Rev. B **69,** 125304 (2004).
[29] C. Delerue, G. Allan, amd Y.M. Niquet, Phys. Rev. B **72,** 195316 (2004).
[30] L.W. Wang and A. Zunger, J. Phys. Chem. B **102,** 6449 (1998).
[31] A. Franceschetti, H. Fu, L. Wang, and A. Zunger, Phys. Rev. B **60,** 1819 (1999).
[32] M. Califano, A. Franceschetti, and A. Zunger, Phys. Rev. B **75,** 115401 (2007).
[33] R.D. Schaller and V.I. Klimov, Phys. Rev. Lett. **92,** 186601 (2004).
[34] A.J. Nozik, Chem. Phys. Lett. **457,** 3 (2008).
[35] R.D. Schaler, M. Sykora, J.M. Pietryga, and V.I. Klimov, Nano Lett. **6,** 424 (2006).
[36] A. Pandey and P. Guyot-Sionnest, J. Chem. Phys. **127,** 111104 (2007)
[37] A.J. Nozik, Annu. Rev. Phys. Chem. **52,** 193 (2001).
[38] A. Shabaev, Al.L. Efros, and A.J. Nozik, Nano Lett. **6,** 2856 (2006).
[39] R.D. Schaller, V.M. Agranovich, and V.I. Klimov, Nature Phys. **1,** 189 (2005).
[40] G. Allan and C. Delerue, Phys. Rev. B **73,** 205423 (2006).
[41] G. Allan and C. Delerue, Phys. Rev. B **77,** 125340 (2008).
[42] M. Califano, ACS Nano **3,** 2706 (2009).
[43] W.M. Witzel, A. Shabaev, C.S. Hellberg, V.L. Jacobs, and A.L. Efros, Phys. Rev. Lett. **105,** 137401 (2010).
[44] S.V. Kilina, D.S. Kilin, and O.V. Prezhdo, ACS Nano **3,** 93 (2009).
[45] O.V. Prezhdo, Acc. Chem. Res. **42,** 2005 (2009).
[46] P. Hawrylak, A. Wojs, and J. A. Brum, Phys. Rev. B **54,** 11397 (1996).
[47] M. Korkusinski, O. Voznyy, and P. Hawrylak, Phys. Rev. B **82,** 245304 (2010).
[48] M. Korkusinski, M. Zielinski, and P. Hawrylak, J. Appl. Phys. **105,** 122406 (2009).
[49] S. Lee, F. Oyafuso, P. von Allmen, and G. Klimeck, Phys. Rev. B **69,** 045316 (2003).
[50] J. C. Slater, Phys. Rev. **36,** 57 (1930).
[51] L.W. Wang, M. Califano, A. Zunger, and A. Franceschetti, Phys. Rev. Lett. **91,** 056404 (2003).
[52] I. Moreels, G. Allan, B. De Geyter, L. Wirtz, C. Delerue, and Z. Hens, Phys. Rev. B **81,** 235319 (2010).
[53] S. Ogut, R. Burdick, Y. Saad, and J.R. Chelikovsky, Phys. Rev. Lett. **90,** 127401 (2003).
[54] C. Delerue, M. Lannoo, and G. Allan, Phys. Rev. B **68,** 115411 (2003).